Subcortical brain structure segmentation using FCNNs

Stavros Tsogkas[1], *Mahsa Shakeri[2,3], Enzo Ferrante[1], Sarah Lippe[3,4], Samuel Kadoury[2,3], Nikos Paragios[1], Iasonas Kokkinos[1]*

CentraleSupélec
1

POLYTECHNIQUE MONTRÉAL
2

CHU Sainte-Justine
3

Université de Montréal
4

Diseases and their relation to subcortical structures

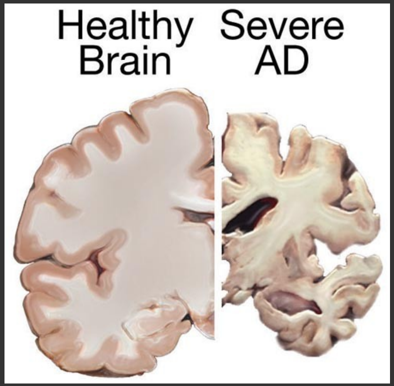

Alzheimer's:
structure degeneration

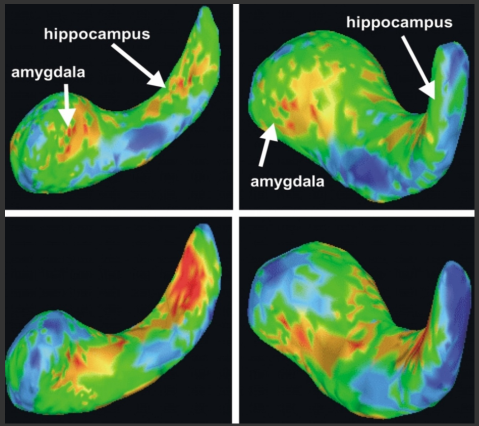

Schizophrenia: volume abnormalities
[Shenton M.E. et al., Psychiatry Res. 2002]

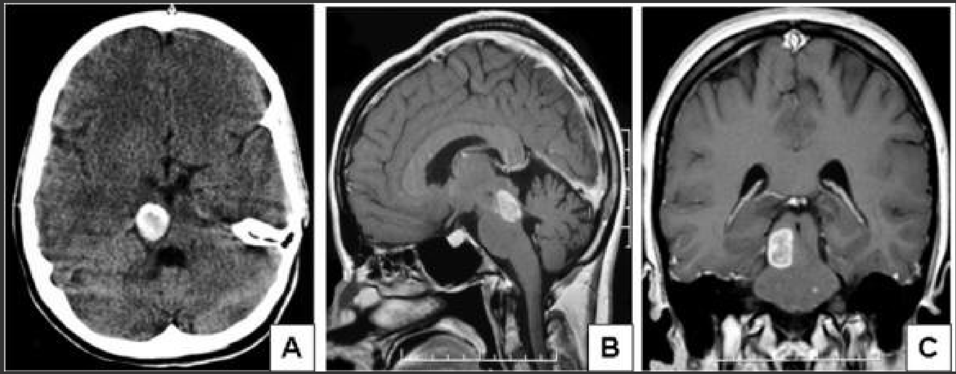

Tumors: avoid radiation on sensitive regions
[Hoehn D. et al., Journal of Medical Cases, 2012]

3D Segmentation

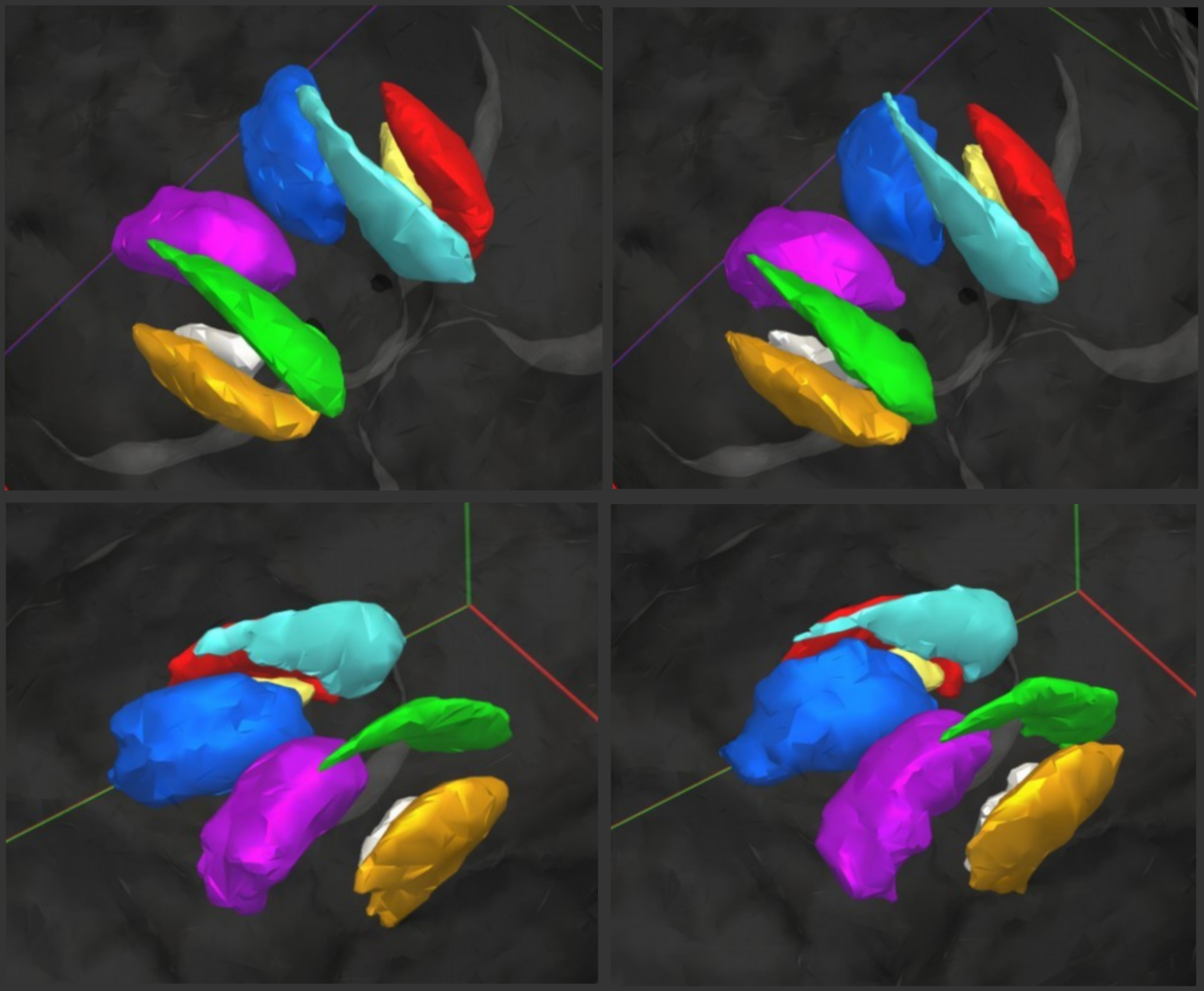

Our results Groundtruth

Why automatic segmentation?

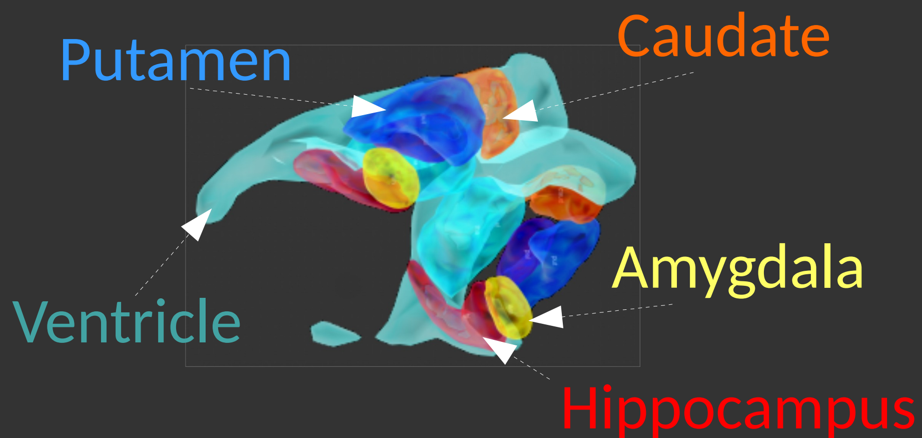

Visualization and inspection

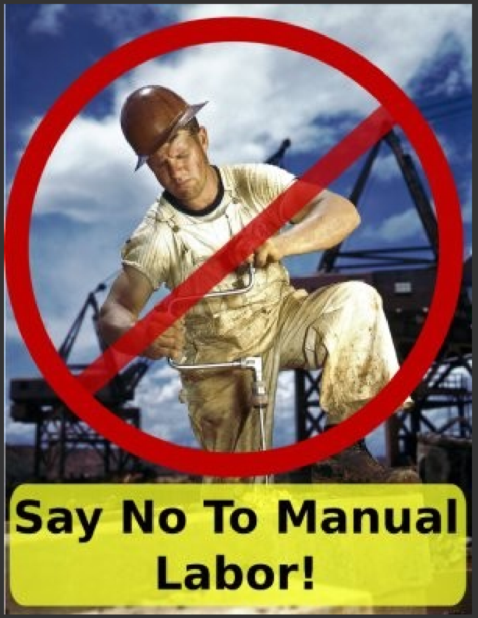

No need for manual annotation (time consuming, need experts, limited reproducibility)

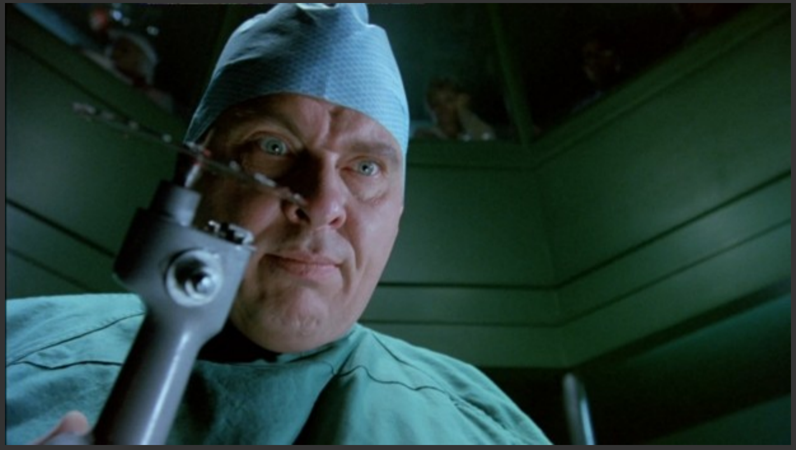

Non-invasive diagnosis and treatment

Segmentation using MRI

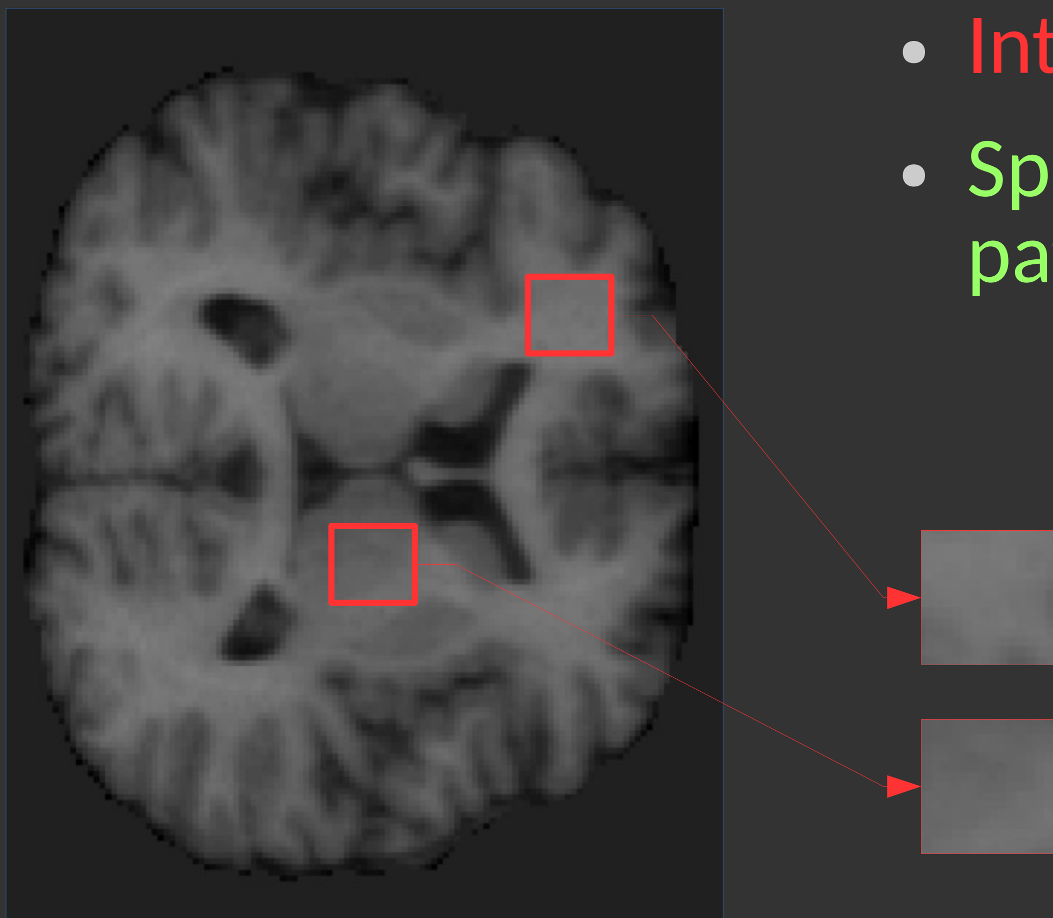

- Intensity is not enough
- Spatial arrangement patterns

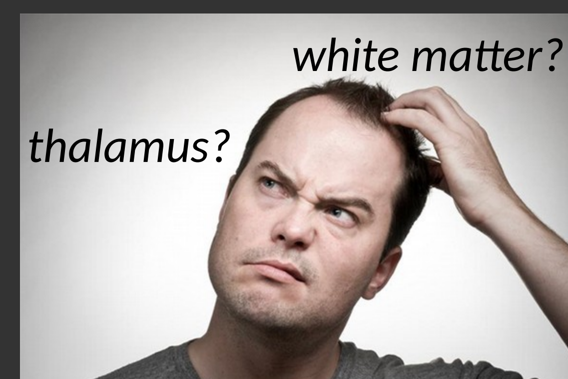

Goal

- Classify *every pixel* as one of *L* possible structures.
- Exploit context.
- Enforce volumetric homogeneity.

Fully convolutional neural networks (FCNNs)
+ Graphical models (MRFs)

Outline

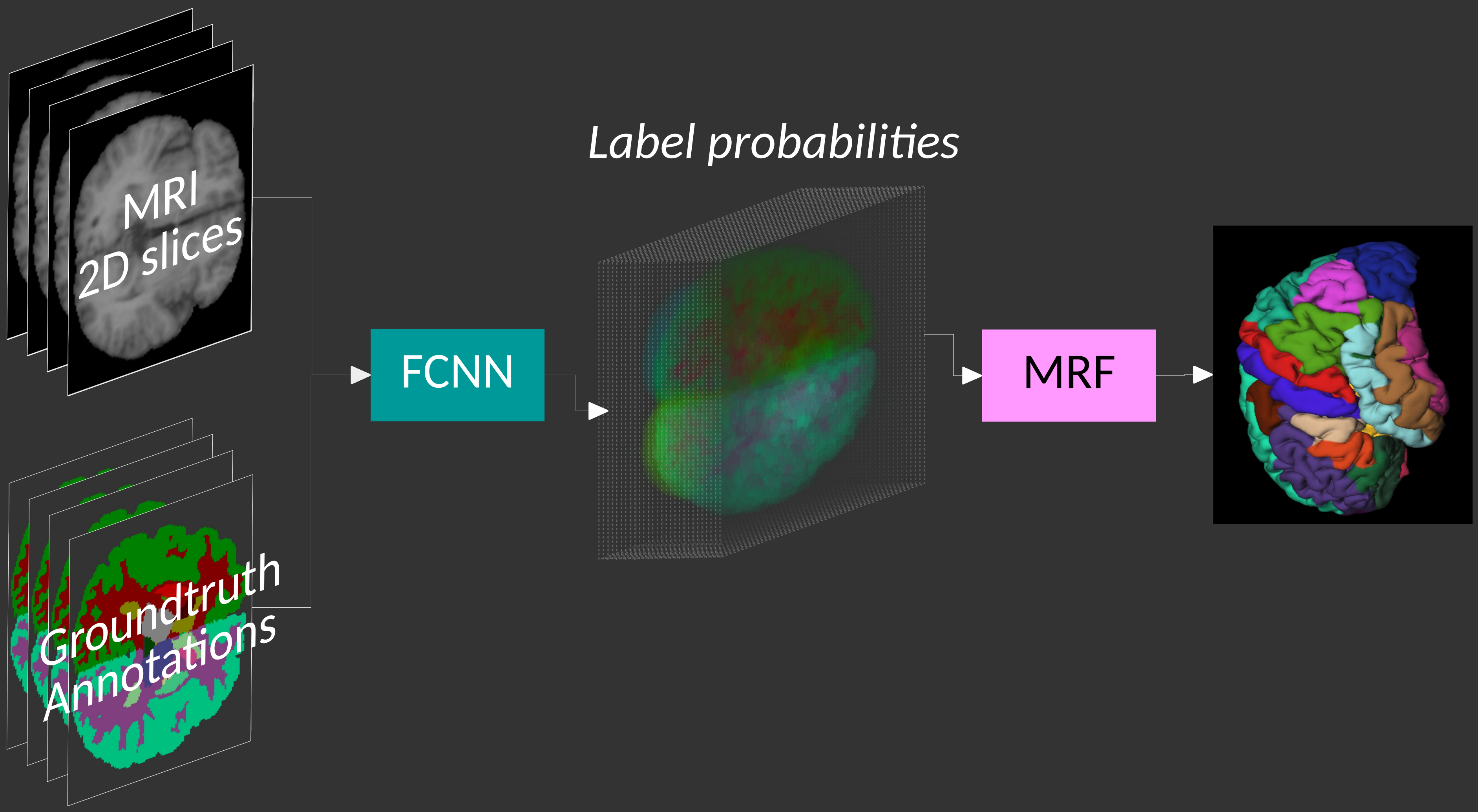
MRI
2D slices
Groundtruth
Annotations
FCNN
Label probabilities
MRF

Semantic segmentation of MRI slices

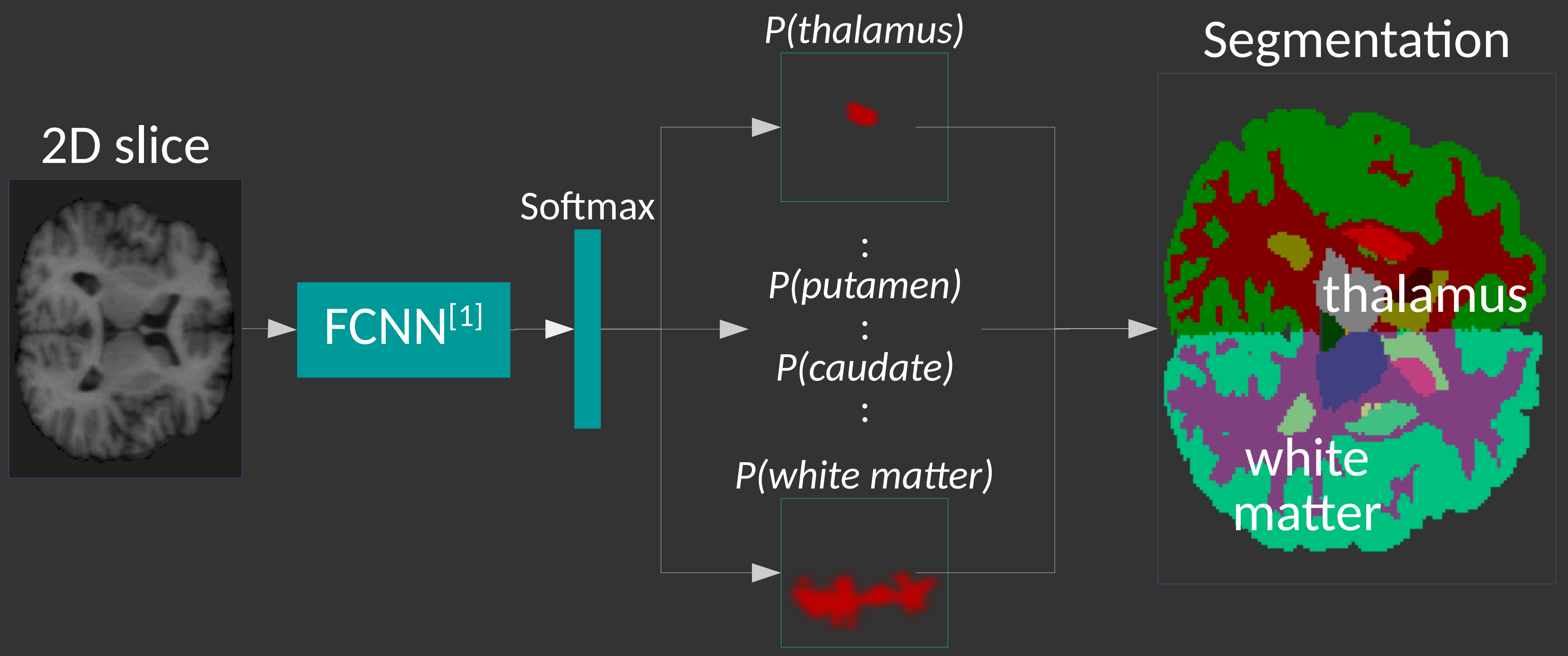

[1] Long et al., CVPR 2015

Our CNN architecture

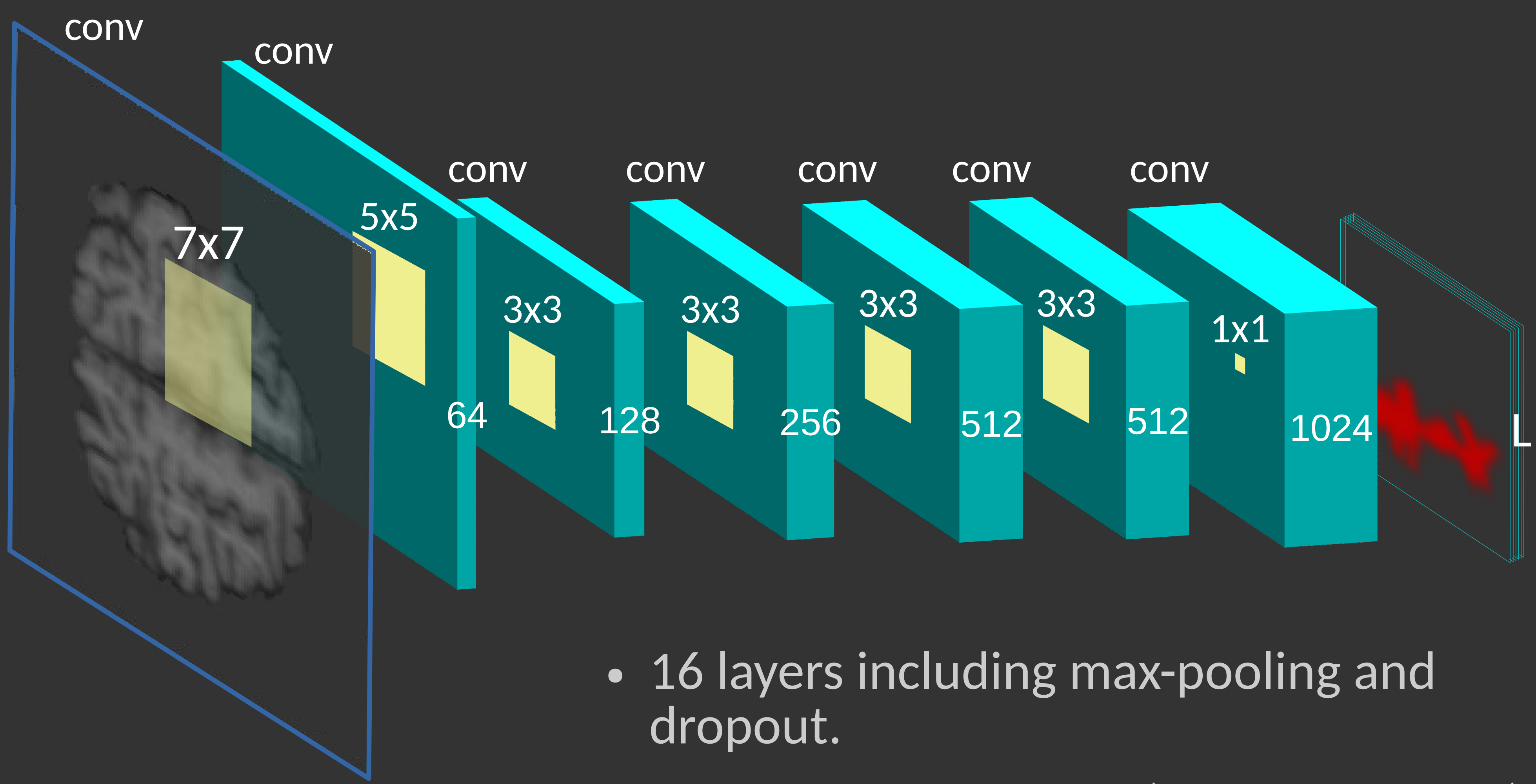

- 16 layers including max-pooling and dropout.
- Compact architecture *(~4GB GPU RAM)*.

MRF for volume homogeneity

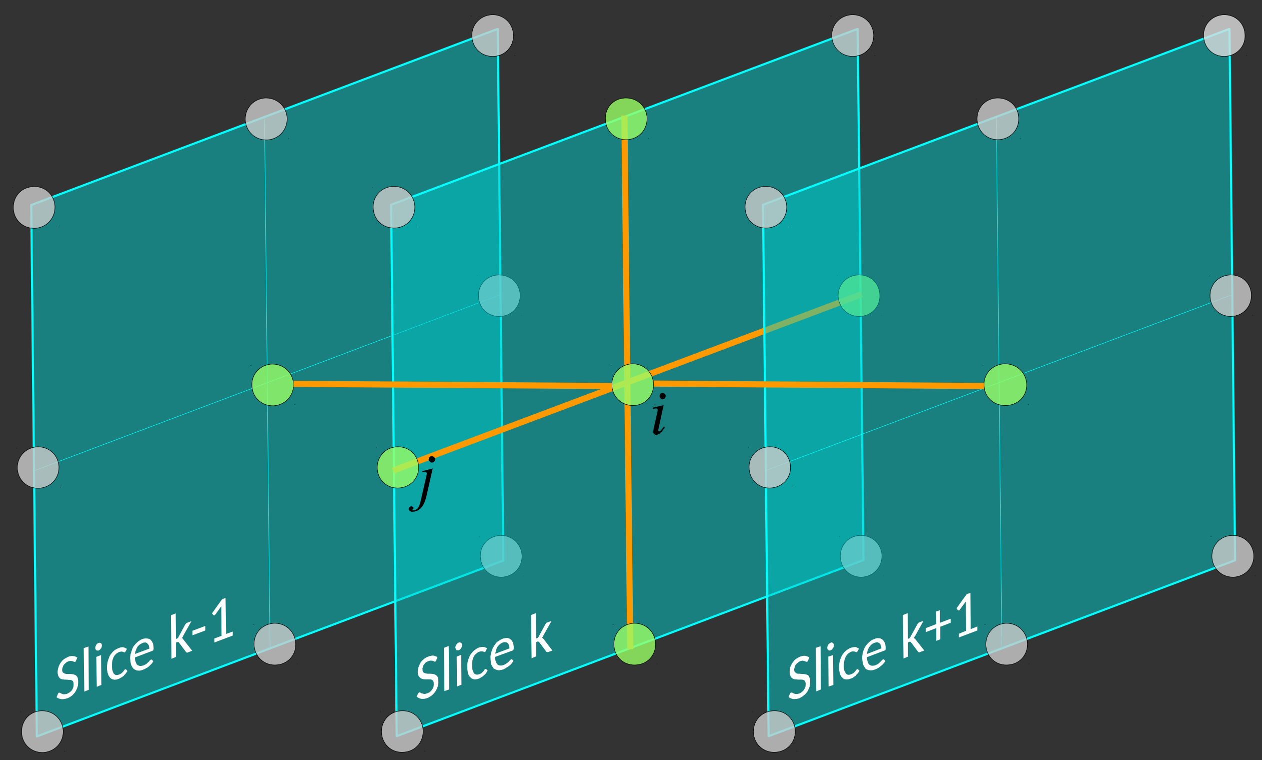

$$\mathcal{S}^* = \mathrm{argmin} E(\mathcal{S}) = \sum_{i \in \mathcal{V}} \underbrace{V_i(l_i)}_{f(P_i^{\mathrm{CNN}}(l_i))} + \lambda \sum_{(i,j) \in \mathcal{E}} \underbrace{V_{ij}(l_i, l_j)}_{d(I_i, I_j)[l_i \neq l_j]}$$

Experiments

- Two datasets:
  - Internet Brain Segmentation Repository (IBSR).
  - Roland Epilepsy (RE).
- Train CNN on 2D slices from *axial* view.
- Data augmentation: ~100K training images.

Results (Dice coefficient)

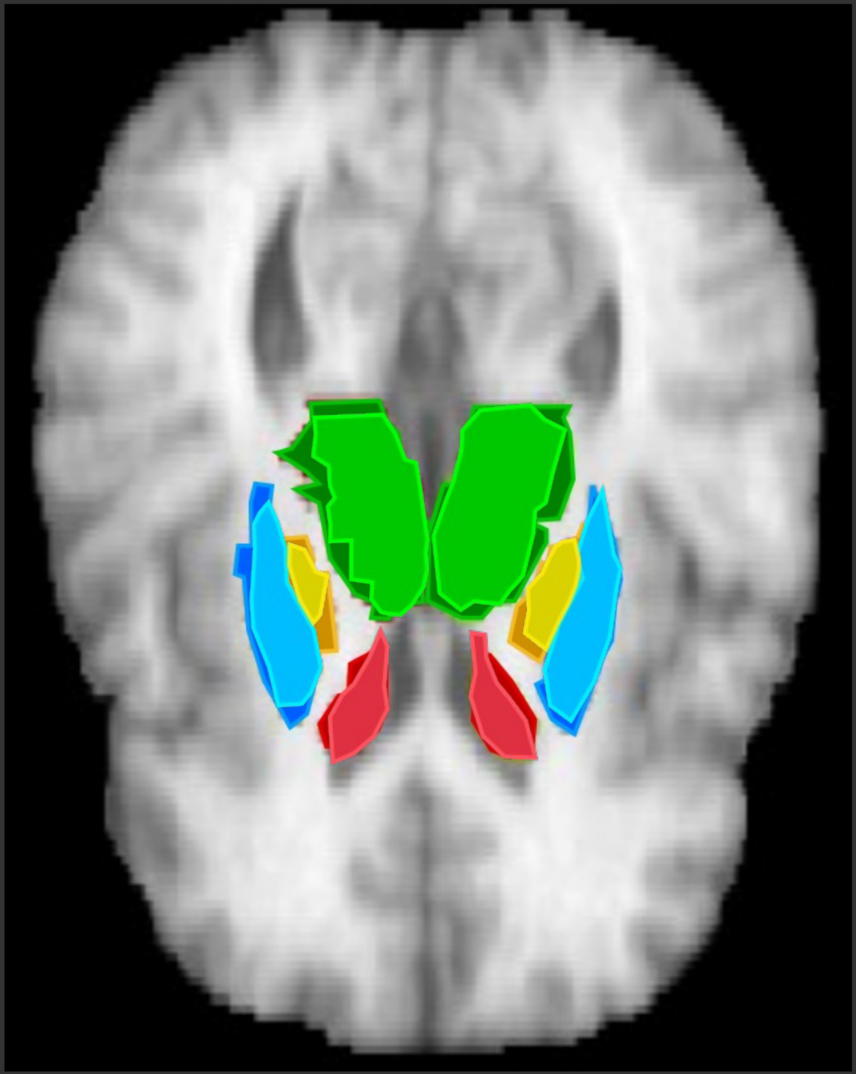

Dice: 1 = perfect overlap with ground truth.

Average Dice (IBSR)

- Thalamus: 0.87
- Putamen: 0.83
- Caudate: 0.78
- Pallidum: 0.75

Comparison with other methods

Dice coefficient

	Freesurfer[1]	FSL[2]	Ours
IBSR - Thalamus	0.86	0.85	**0.87**
IBSR - Caudate	**0.82**	0.68	0.78
IBSR - Putamen	0.81	0.81	**0.83**
IBSR - Pallidum	0.71	0.73	**0.75**
RE - Putamen	0.74	0.88	**0.89**
Running time (1 vol.)	~hours	~minutes	**~1 minute**

[1] Fischl et al., Neuron 2002.

[2] Patenaude et al., NeuroImage 2011.

The type of unaries matters

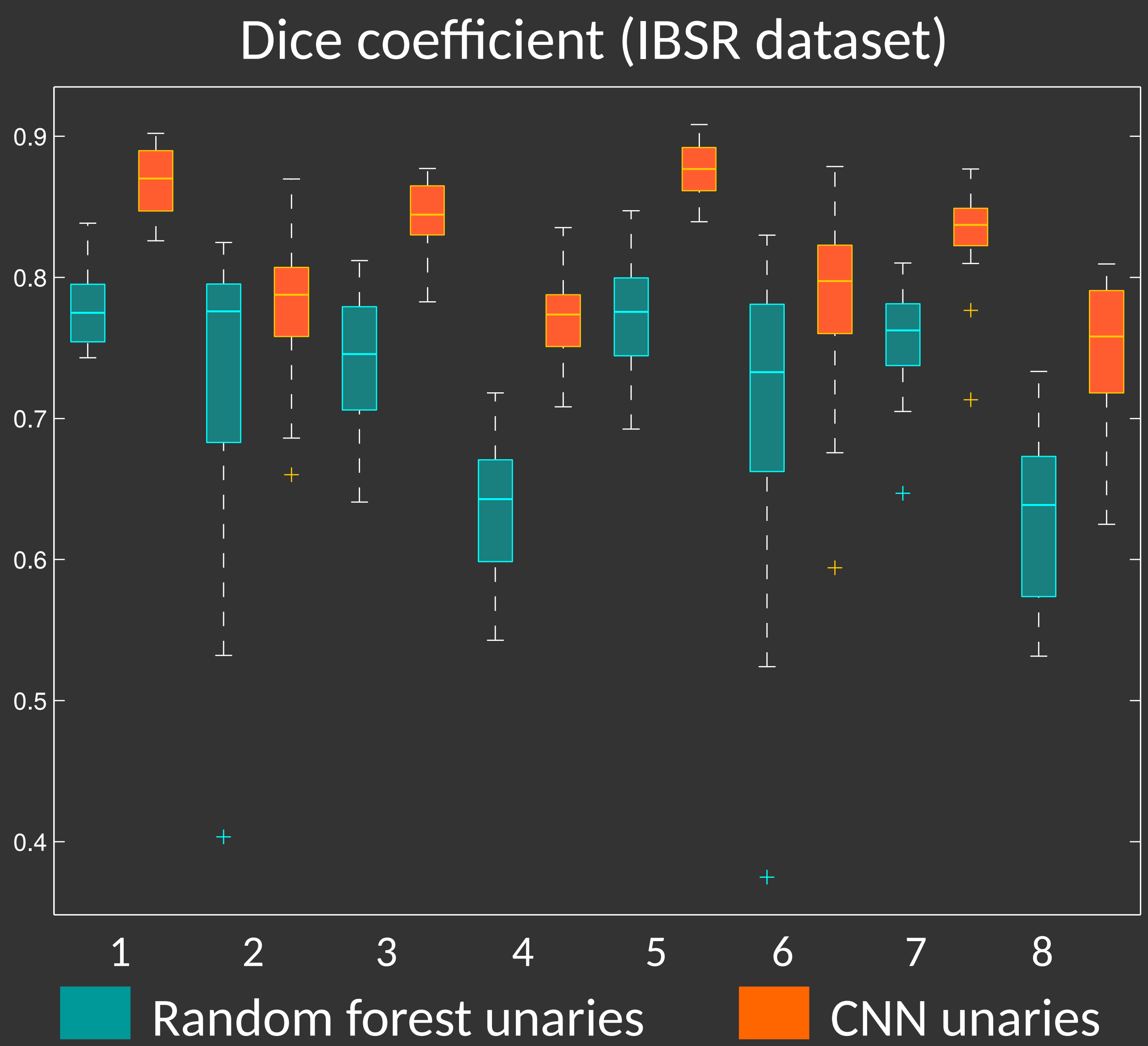

1. Thalamus left
2. Caudate left
3. Putamen left
4. Pallidum left
5. Thalamus right
6. Caudate right
7. Putamen right
8. Pallidum right

The type of unaries matters

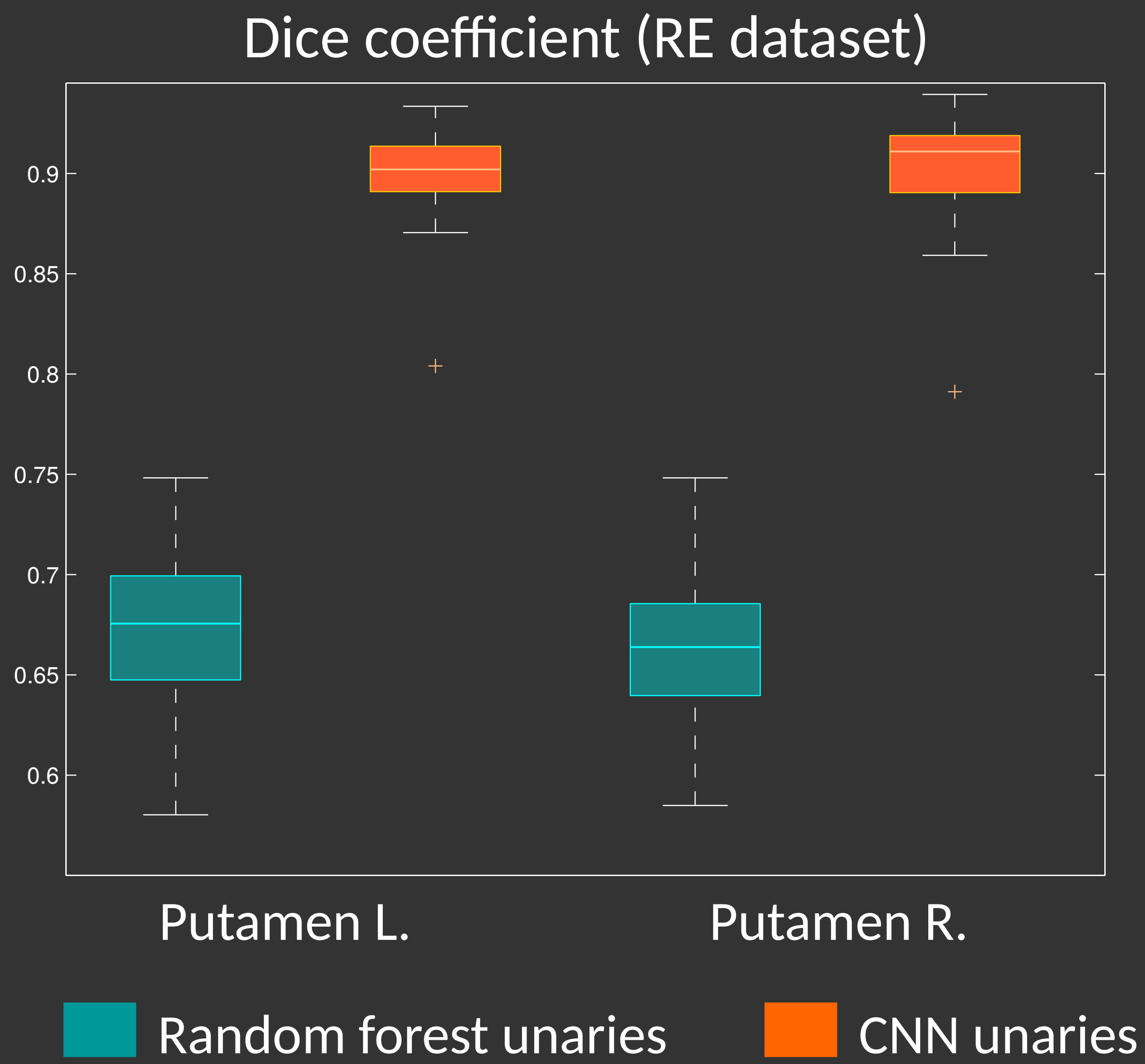

MRF removes spurious responses

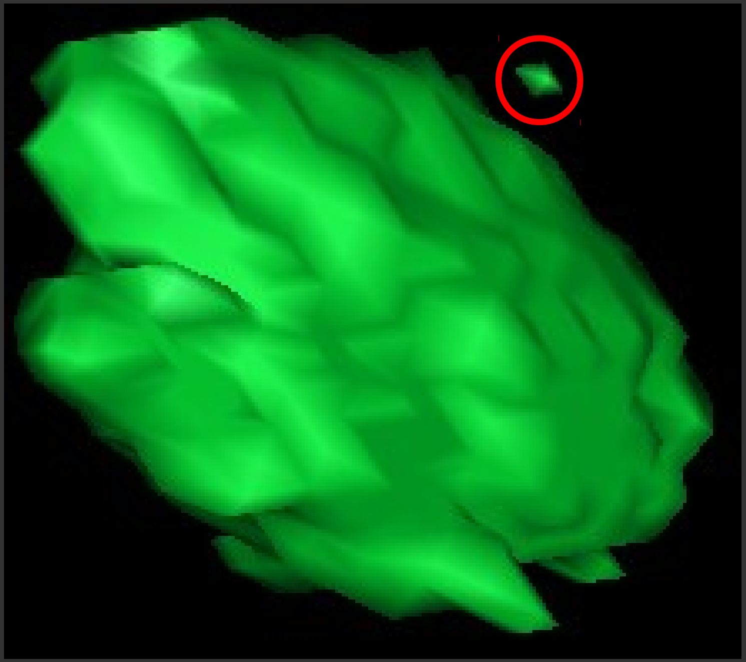
CNN

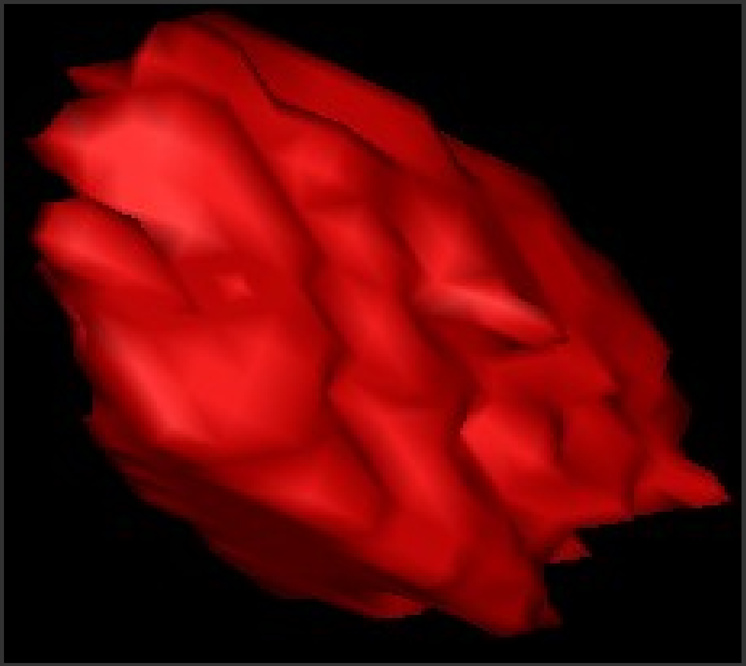
CNN+MRF

Limitations and future directions

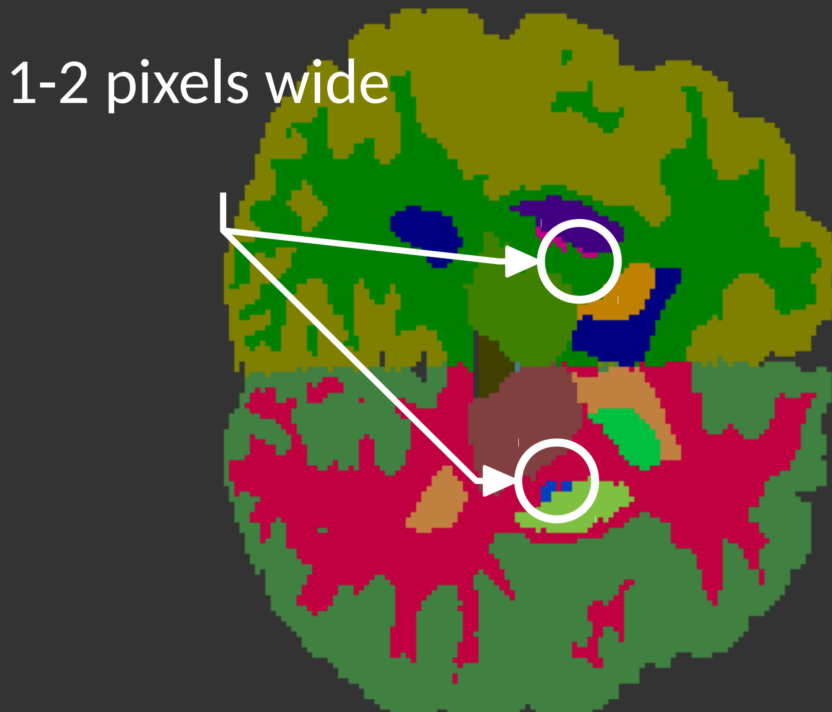

Small structures are challenging

Left hemisphere Right hemisphere

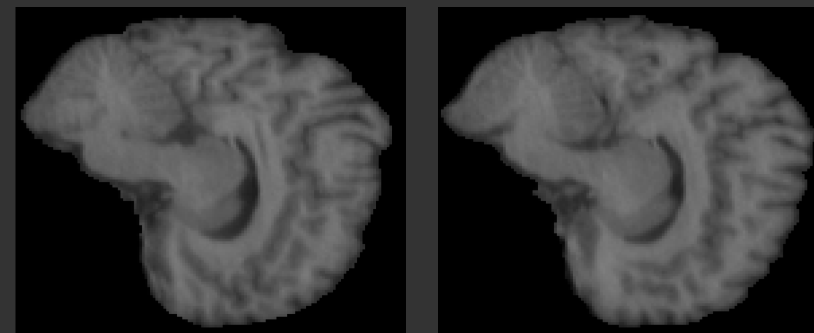

Does not work for sagittal view because of symmetry

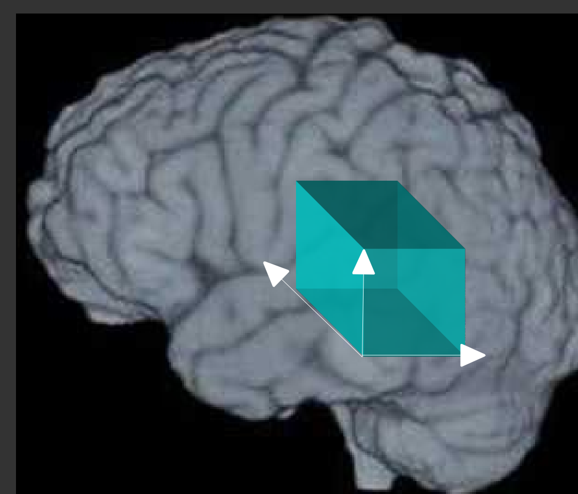

3D CNNs

Summary

- FCNNs + MRFs:
  - accurate, *dense* labelling using 2D image data.
  - volumetric homogeneity
- Efficient segmentation of 3D volumes: *(~1 min)*
- No need for expensive GPUs *(~4GB GPU RAM)*

Code, CNN probability maps:
https://github.com/tsogkas/brainseg

CentraleSupélec · Inria · Polytechnique Montréal · CHU Sainte-Justine · Université de Montréal · Mitacs Globalink

IBSR dataset: Hausdorff distance

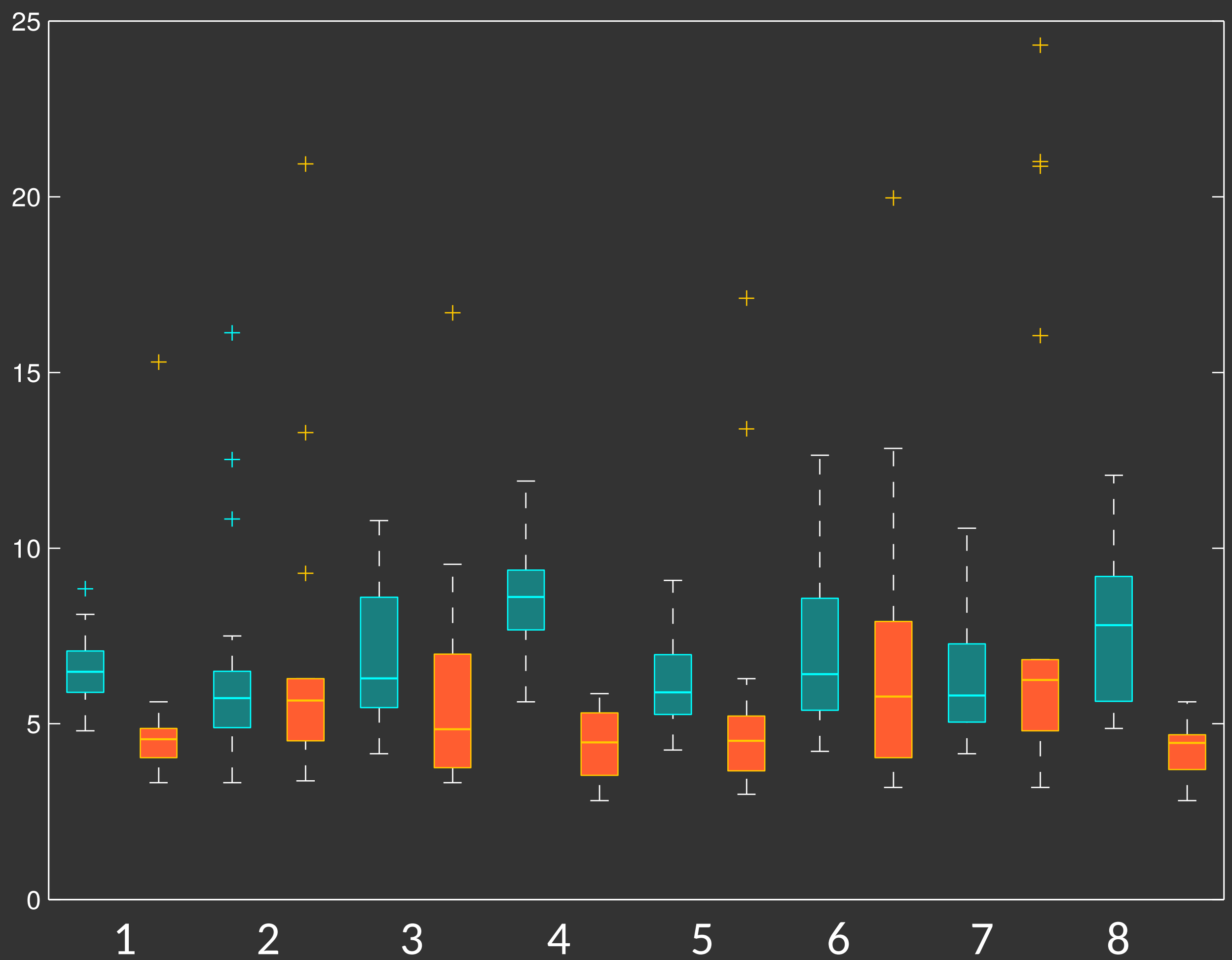

1. Thalamus left
2. Caudate left
3. Putamen left
4. Pallidum left
5. Thalamus right
6. Caudate right
7. Putamen right
8. Pallidum right

Random forest unaries

CNN unaries

IBSR dataset: contour mean distance

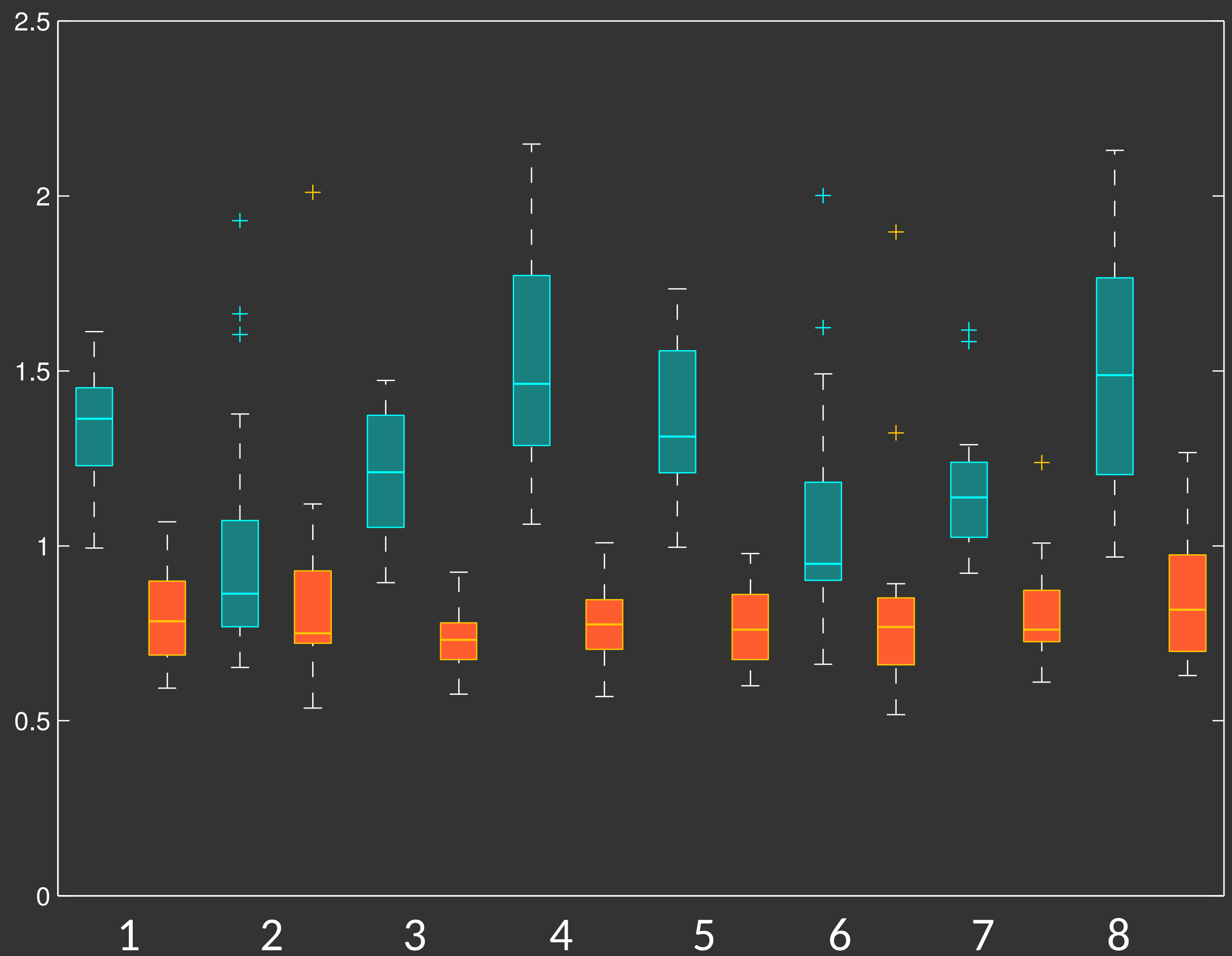

1. Thalamus left
2. Caudate left
3. Putamen left
4. Pallidum left
5. Thalamus right
6. Caudate right
7. Putamen right
8. Pallidum right

Random forest unaries CNN unaries

RE dataset: HD and CMD